

Formation of Novel *ansa*-Carborane–Alkoxide Complexes by Carbonylation of $(\text{C}_5\text{Me}_5)(\eta^5\text{-C}_2\text{B}_9\text{H}_{11})\text{TiMe}$

Xiaohong Bei, Carsten Kreuder, Dale C. Swenson, and Richard F. Jordan*

Department of Chemistry, The University of Iowa, Iowa City, Iowa 52242

Victor G. Young, Jr.

Department of Chemistry, The University of Minnesota, Minneapolis, Minnesota 55455

Received November 4, 1997

The reaction of $\text{Cp}^*(\eta^5\text{-C}_2\text{B}_9\text{H}_{11})\text{TiMe}$ (**1**, $\text{Cp}^* = \text{C}_5\text{Me}_5$) with CO (0.5–1 atm) in toluene (–78 to 23 °C) yields a 1:4 mixture of $\text{Cp}^*(\eta^5:\eta^1\text{-8-CHMeO-C}_2\text{B}_9\text{H}_{10})\text{Ti}$ (**6**) and $\text{Cp}^*(\eta^5:\eta^1\text{-4-CHMeO-C}_2\text{B}_9\text{H}_{10})\text{Ti}$ (**7**), in ca. 90% total NMR yield. Complexes **6** and **7** both contain a linked carborane–alkoxide ligand but differ in the site of attachment of the –CHMeO– linker to the carborane cage. The linker is attached at the central boron of the C_2B_3 donor ring (B8) in **6** and to a lateral boron (B4 or B7) in **7**. The anticipated acyl complex, $\text{Cp}^*(\eta^5\text{-C}_2\text{B}_9\text{H}_{11})\text{TiC(=O)Me}$ (**8**), was not observed. However, experiments with ^{13}CO show that the –BCHMeO– carbon atoms in **6** and **7** originate from the CO, which implies that **8** is formed first and rearranges to **6** or **7** by net insertion of the acyl carbon into a B–H bond. The molecular structures of **6** and $\text{Cp}^*(\eta^5:\eta^1\text{-4-CHMeO-C}_2\text{B}_9\text{H}_{10})\text{Ti(NCMe)}$ (**9**) have been determined by X-ray crystallography.

Introduction

The methane elimination reaction of Cp^*TiMe_3 ($\text{Cp}^* = \text{C}_5\text{Me}_5$) and $\text{C}_2\text{B}_9\text{H}_{13}$ yields the bent metallocene complex $\text{Cp}^*(\eta^5\text{-C}_2\text{B}_9\text{H}_{11})\text{TiMe}$ (**1**, Chart 1), which is isostructural and isolobal with group 4 metal Cp_2MR^+ complexes (**2**) and displays many of the same reactivity properties.^{1,2} Complex **1** forms adducts with Lewis bases, inserts 2-butyne and acetonitrile, and undergoes intramolecular C–H activation to yield bent metallocenes **3–5**. However, the effective charge at the metal center is lower for neutral **1** than for cationic **2**, which gives rise to important reactivity differences. For example, while Cp_2TiR^+ species polymerize ethylene,^{3–6} **1** only dimerizes this substrate because the key intermediate $(\text{Cp}^*)(\eta^5\text{-C}_2\text{B}_9\text{H}_{11})\text{TiBu}$ undergoes $\beta\text{-H}$ elimination much faster than it inserts ethylene.^{1a}

(1) (a) Kreuder C.; Jordan, R. F.; Zhang, H. *Organometallics* **1995**, *14*, 2993. For analogous Zr and Hf chemistry, see: (b) Crowther, D. J.; Swenson, D. C.; Jordan, R. F. *J. Am. Chem. Soc.* **1995**, *117*, 10403. (c) Crowther, D. J.; Baenziger, N. C.; Jordan, R. F. *J. Am. Chem. Soc.* **1991**, *113*, 1455. (d) Crowther, D. J.; Jordan, R. F. *Makromol. Chem., Macromol. Symp.* **1993**, *66*, 121. (e) Yoshida, M.; Crowther, D. J.; Jordan, R. F. *Organometallics* **1997**, *16*, 1349. (f) Yoshida, M.; Jordan, R. F. *Organometallics* **1997**, *16*, 4508.

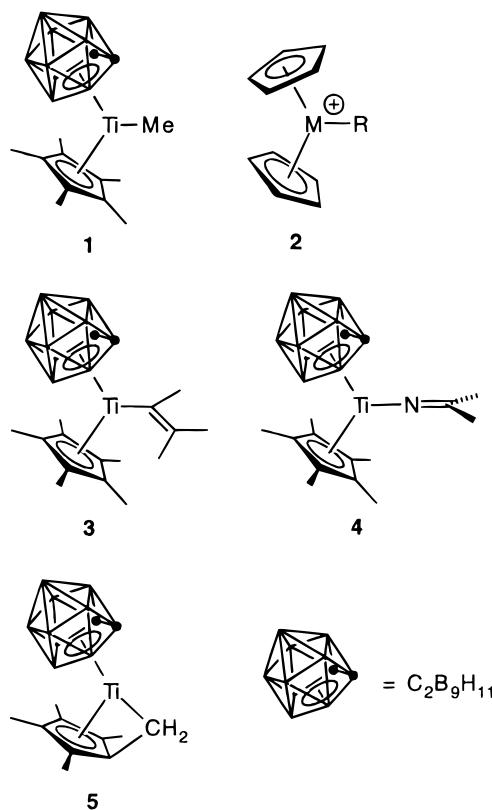
(2) For reviews concerning the chemistry of cationic group 4 metallocene complexes, see: (a) Guram, A. S.; Jordan, R. F. In *Comprehensive Organometallic Chemistry II*; Abel, E. W., Stone, F. G. A., Wilkinson, G., Eds.; Elsevier: Oxford, 1995; Vol. 4, p 589. (b) Bochmann, M. *J. Chem. Soc., Dalton Trans.* **1996**, 255. (c) Horton, A. D. *Trends Polym. Sci.* **1994**, *2*, 158. (d) Marks, T. J. *Acc. Chem. Res.* **1992**, *25*, 57. (e) Jordan, R. F. *Adv. Organomet. Chem.* **1991**, *32*, 325. (f) Jordan, R. F.; Bradley, P. K.; Lapointe, R. E.; Taylor, D. F. *New J. Chem.* **1990**, *14*, 505.

(3) For a review, see: Möhring, P. C.; Coville, N. J. *J. Organomet. Chem.* **1994**, *479*, 1.

(4) Mallin, D. T.; Rausch, M. D.; Mintz, E. A.; Rheingold, A. L. *J. Organomet. Chem.* **1990**, *381*, 35.

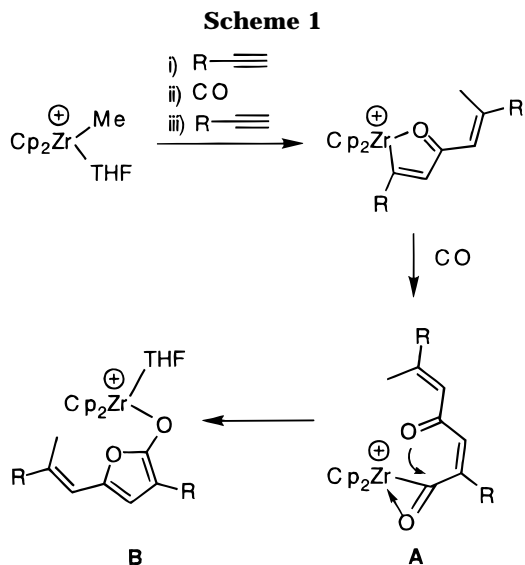
(5) (a) Ewen, J. A. *J. Am. Chem. Soc.* **1984**, *106*, 6355. (b) Ewen, J. A. *Stud. Surf. Sci. Catal.* **1986**, *25*, 271. (c) Giannetti, E.; Nicoletti, G. M.; Mazzocchi, R. *J. Polym. Sci., Polym. Chem. Ed.* **1985**, *23*, 2117.

Chart 1



In other work, we have shown that $\text{Cp}_2\text{Zr(Me)(THF)}^+$ undergoes alternating insertion of alkynes and CO,

(6) However, the discrete cationic systems $[\text{Cp}^*_2\text{Ti(Me)}][\text{BPh}_4]$ and $[\text{Cp}^*_2\text{Ti(Me)}(\text{tetrahydrothiophene})][\text{BPh}_4]$ are reported to be inactive with ethylene, see: (a) Bochmann, M.; Jagggar, A. J. *J. Organomet. Chem.* **1992**, *424*, C5. (b) Eshuis, J. J. W.; Tan, Y. Y.; Teuben, J. H.; Renkema, J. *J. Mol. Catal.* **1990**, *62*, 277.



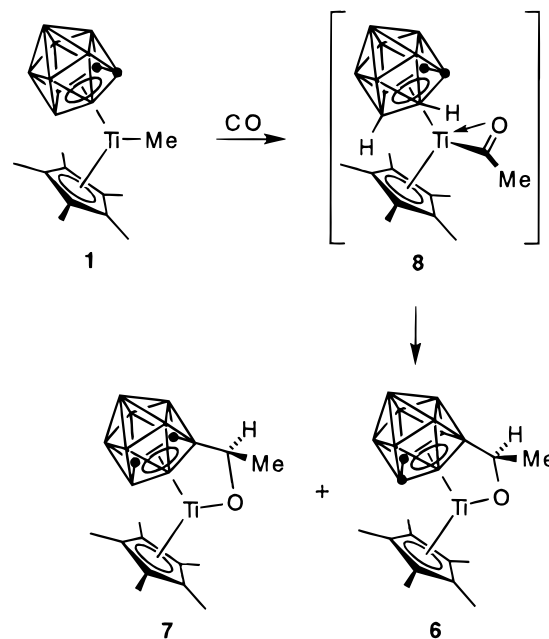
yielding interesting η^2 - β -keto-alkenyl and η^2 - α , β -unsaturated acyl species (Scheme 1).⁷ However, intermediate **A**, which is generated by the second CO insertion, rearranges by nucleophilic attack of the remote carbonyl group on the η^2 -acyl carbon, ultimately yielding zirconoxyfuran product **B**. This cyclization reaction limits the degree of alkyne/CO co-oligomerization which can be achieved in this system. In considering strategies for disfavoring rearrangements of this type, we reasoned that the lower metal charge of Cp^* -(η^5 - $\text{C}_2\text{B}_9\text{H}_{11}$)MC(=O)R acyl species should result in a weaker M–O interaction, a corresponding decrease in the electrophilicity of the acyl carbon, and a reduced tendency for cyclization as compared to analogous Cp_2 -MC(=O)R⁺ species. Here, we describe the initial studies of the carbonylation of **1** and the discovery of an unusual B–H activation reaction which generates novel complexes containing linked carborane–alkoxide ligands.

Results

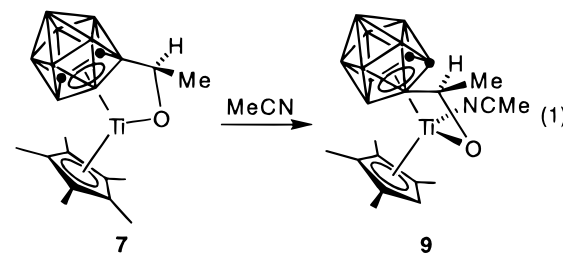
Reaction of $\text{Cp}^*(\eta^5\text{-C}_2\text{B}_9\text{H}_{11})\text{TiMe}$ (**1**) with CO.

The reaction of **1** with CO (0.5–1 atm) in toluene (–78 to 23 °C) yields a mixture of two novel products, $\text{Cp}^*(\eta^5;\eta^1\text{-8-CHMeO-C}_2\text{B}_9\text{H}_{10})\text{Ti}$ (**6**) and $\text{Cp}^*(\eta^5;\eta^1\text{-4-CHMeO-C}_2\text{B}_9\text{H}_{10})\text{Ti}$ (**7**), in ca. 90% total NMR yield (Scheme 2). The **6**:**7** product ratio varies from 1:4 to 1:5. Complexes **6** and **7** both contain a linked carborane–alkoxide ligand but differ in the site of attachment of the –CHMeO– linker to the carborane cage. The linker is attached at the central boron of the C_2B_3 donor ring (B8) in **6** and to a lateral boron (B4 or B7) in **7**. Complexes **6** and **7** do not interconvert under the reaction conditions. Interestingly, only one of the two possible diastereomers is observed for **7**, and in the absence of coordinating solvents or Lewis bases, **7** is partially dimerized while **6** is monomeric (vide infra). The anticipated acyl complex, $\text{Cp}^*(\eta^5\text{-C}_2\text{B}_9\text{H}_{11})\text{TiC}(=\text{O})\text{Me}$ (**8**), was not observed. However, experiments with ^{13}CO show that the –BCHMeO– carbon atoms in **6** and **7** originate from the CO, which implies that **8** is formed first and rearranges to **6** and **7**, as indicated in Scheme 2.

Scheme 2



Separation and Characterization of 6. Initially, characterization of **6** was complicated by the lack of an efficient method to separate **6** and **7**, which have similar solubility properties. However, addition of 1 equiv (vs **7**) of CH_3CN to a 1:1 mixture of **6** and **7** in aromatic solvents causes selective precipitation of $\text{Cp}^*(\eta^5;\eta^1\text{-4-CHMeO-C}_2\text{B}_9\text{H}_{10})\text{Ti}(\text{CH}_3\text{CN})$ (**9**, eq 1), allowing separation of **6**. Crystals of **6** suitable for X-ray analysis were



obtained by recrystallization from benzene/hexanes.

The molecular structure of **6** is shown in Figure 1, and important bond distances and bond angles are listed in Table 1. Compound **6** adopts a three-coordinate bent-metalloocene structure in which the η^5 -dicarbollide ligand is also linked to Ti through a –CHMeO– bridge, which is attached to the central boron of the C_2B_3 face. The Cp^* and dicarbollide ligands are staggered relative to each other, and the BCHMeOTi bridge is located at the front of the metallocene wedge. The alkoxide oxygen atom lies in the equatorial plane of the metallocene and occupies the central coordination site, i.e., the (Cp^* centroid)–Ti–O and (dicarbollide centroid)–Ti–O angles are essentially equal, and the angle between the Ti–O bond and the (Cp^* centroid)–Ti–(dicarbollide centroid) plane is 13.7°. Several metrical parameters associated with the bridge deviate from normal ranges. Specifically, the B(8)–C(6) bond is directed 35.5° out of the C_2B_3 plane toward Ti (ca. 12° greater than normal), the B(8)–C(6)–O(1) angle is unusually small (96.0(9)°), and the C(6)–O(1) bond (1.51(1) Å) is ca. 0.09 Å longer than

(7) (a) Guram, A. S.; Guo Z.; Jordan, R. F. *J. Am. Chem. Soc.* **1993**, *115*, 4902. (b) Guo, Z.; Swenson, D. C.; Guram, A. S.; Jordan, R. F. *Organometallics* **1994**, *13*, 766.

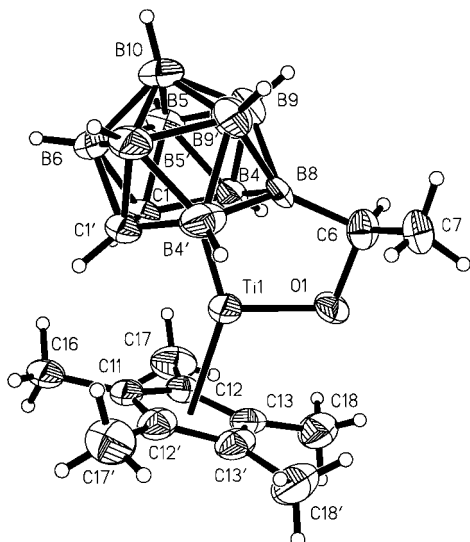


Figure 1. Molecular structure of $\text{Cp}^*(\eta^5:\eta^1\text{-}8\text{-CHMeO-C}_2\text{B}_9\text{H}_{10})\text{Ti}$ (**6**).

Table 1. Selected Bond Lengths (Å) and Angles (deg) for $\text{Cp}^*(\eta^5:\eta^1\text{-}8\text{-CHMeO-C}_2\text{B}_9\text{H}_{10})\text{Ti}$ (6**)^{a,b}**

Ti(1)–cnt(Dc)	1.830	Ti(1)–C(11)	2.398(9)
Ti(1)–cnt(Cp*)	2.041	C(1)–C(1')	1.54(2)
Ti(1)–O(1)	1.879(7)	C(1)–B(4)	1.64(1)
Ti(1)–B(4)	2.28(1)	B(4)–B(8)	1.85(3)
Ti(1)–B(8)	2.32(1)	B(8)–C(6)	1.65(2)
Ti(1)–C(1)	2.359(6)	C(6)–C(7)	1.50(2)
Ti(1)–C(13)	2.365(6)	C(6)–O(1)	1.51(1)
Ti(1)–C(12)	2.357(7)		
O(1)–Ti(1)–cnt(Dc)	106.4	O(1)–C(6)–B(8)	96.0(9)
O(1)–Ti(1)–cnt(Cp*)	106.9	C(7)–C(6)–H(6A)	114.7(7)
cnt(Dc)–Ti(1)–cnt(Cp*)	145.6	O(1)–C(6)–H(6A)	114.7(6)
C(6)–O(1)–Ti(1)	109.5(6)	B(8)–C(6)–H(6A)	114.7(11)
C(7)–C(6)–O(1)	108.8(10)		

^a Symmetry transformations used to generate equivalent atoms = $-x + 1, y, z$. ^b The centroids of the Cp* and dicarbollide rings are denoted by cnt(Cp*) and cnt(Dc), respectively.

normal.⁸ Thus, the chelate linker must be somewhat strained. The Ti–O distance (1.879(7) Å) is similar to the Ti–O distances observed in $\text{Cp}_2\text{Ti(IV)}$ alkoxide compounds (e.g., $\text{Cp}_2\text{Ti}(\text{OCH}=\text{CH}_2)_2$ 1.903(2) Å; $\text{Cp}_2\text{-TiCl}(\text{OEt})$ 1.855(2) Å) but longer than distances observed in more highly electron-deficient mono-Cp Ti(IV) alkoxides (e.g., $\{\text{C}_5\text{Me}_4(\text{CH}_2)_3\text{O}\}\text{TiCl}_2$ 1.767(1) Å; $\text{CpTiCl}_2\text{-OCMe}_2\text{CMe}_2\text{OTiCl}_2\text{Cp}$ 1.750(2) Å).^{8a,9} The metallocene framework of **6** is structurally very similar to that of **4**. The centroid–Ti–centroid angle (**6**, 145.6°; **4**, 144.6°) and the Ti–Cp* centroid distances (**6**, 2.04 Å; **4**, 2.07 Å) are very similar for the two compounds. The Ti–dicarbollide centroid distance of **6** (1.83 Å) is 0.08 Å shorter than that of **4**, which reflects a slight shortening of the Ti–B bonds (average Ti–B distances **6**, 2.30(2) Å; **4**, 2.40(3) Å) due to the effect of the bridge.

(8) For comparison, TiO–C distances (Å) in representative Ti(IV) alkoxide complexes are as follows: (a) $\text{Cp}_2\text{TiCl}(\text{OEt})$, 1.415(4). See: Huffman, J. C.; Moloy, K. G.; Marsella, J. A.; Caulton, K. G. *J. Am. Chem. Soc.* **1980**, *102*, 3009. (b) $\{\text{PhC}(\text{O})\text{CHC}(\text{O})\text{CF}_3\}_2\text{Ti}(\text{OEt})_2$, 1.434(6). See: Wang, J. L.; Miao, F. M.; Fan, X. J.; Feng, X.; Wang, J. T. *Acta Crystallogr.* **1990**, *C46*, 1633. (c) $\{\text{PhC}(\text{O})\text{CHC}(\text{O})\text{Me}\}_2\text{Ti}(\text{O}^i\text{Bu})_2$, 1.42(1). See: Schubert, U.; Buhler, H.; Hirle, B. *Chem. Ber.* **1992**, *125*, 999.

(9) (a) Curtis, M. D.; Thanedar, S.; Butler, W. M. *Organometallics* **1984**, *3*, 1855. (b) Fandos, R.; Meetsma, A.; Teuben, J. H. *Organometallics* **1991**, *10*, 59.

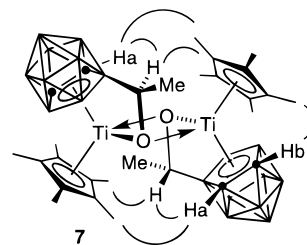


Figure 2. Proposed dimeric structure of $\{\text{Cp}^*(\eta^5:\eta^1\text{-}4\text{-CHMeO-C}_2\text{B}_9\text{H}_{10})\text{Ti}\}_2$ (**7**). Key NOESY correlations discussed in the text are indicated by curved lines.

The solution NMR properties of **6** are consistent with the solid-state structure. The ^{11}B NMR spectrum (C_6D_6) contains seven resonances in a 1:1:1:2:1:2:1 intensity ratio, consistent with a C_1 -symmetric structure, assuming accidental overlap of several resonances. The lowest field resonance (δ 11.9, 1B) does not split in the ^1H -coupled ^{11}B NMR spectrum, indicating that the corresponding B atom does not have a hydrogen substituent. The δ 11.9 resonances exhibits strong ^{11}B – ^{11}B COSY correlations with the 1B resonances at δ 4.8 and 2.6 (B4, B4'), and a medium intensity correlation with the 2B resonance at δ –2.7 (B9, B9') and is, therefore, assigned to the central B atom of the C_2B_3 ring (B8).¹⁰ The ^{13}C NMR spectrum (CD_2Cl_2) of **6** contains a broad resonance at δ 86, which is assigned to the –BCHMeO– carbon. The chemical shift of this resonance is similar to those observed for Ti–O–C carbons (ca. δ 76–86) in $\text{Cp}_2\text{Ti(IV)}$ alkoxide complexes,¹¹ and the broadening is consistent with the direct bonding of this carbon to a B which is in an unsymmetrical environment. The ^1H NMR spectrum of complex **6** exhibits one Cp* resonance, two broad dicarbollide CH resonances, and a set of CHMe resonances.

Characterization of 7. Complex **7** could not be isolated free of **6**. Cryoscopic molecular weight measurements on benzene solutions containing mixtures of **6** and **7** indicate that **7** is substantially dimerized in this solvent ($\text{MW}_{\text{obsd}} = 584(30)$; $\text{MW}_{\text{calcd}} = 358$). NMR data are consistent with the C_7 -symmetric dimer structure in Figure 2, in which two C_1 -symmetric monomer units are linked by alkoxide bridges in an anti arrangement. The ^1H NMR spectrum (C_6D_6 or toluene- d_8) of **7** contains one Cp* resonance, two broad dicarbollide CH resonances, and a doublet and a broad quartet for the –BCHMeO– hydrogens. The ^{13}C NMR spectrum ($\text{CD}_2\text{-Cl}_2$) contains a broad signal at δ 83 for the alkoxide carbon and two broad signals at δ 60.2 and 58.6 for the dicarbollide carbons. The ^{11}B NMR spectrum (C_6D_6) contains seven resonances in a 1:2:1:1:2:1:1 intensity ratio. The ^{11}B NMR spectrum in THF- d_8 is similar (1:1:2:1:2:1:1 intensity pattern), and in this solvent one

(10) If the δ 11.9 resonance was due to one of the lateral borons B4 or B4', one strong and one medium intensity cross-peak would be expected; the B4–B5 cross-peak is expected to be weak or undetectable because both of these borons are bonded to a cage carbon, see: (a) Venable, T. L.; Hutton, W. C.; Grimes, R. N. *J. Am. Chem. Soc.* **1984**, *106*, 29. (b) Uhrhammer, R.; Su, Y.-X.; Swenson, D. C.; Jordan, R. F. *Inorg. Chem.* **1994**, *33*, 4398. (c) Brown, M.; Plessek, J.; Base, K.; Stibr, B.; Fontaine, X. L. R.; Greenwood, N. N.; Kennedy, J. D. *Magn. Reson. Chem.* **1989**, *27*, 947. (d) Fontaine, X. L. R.; Greenwood, N. N.; Kennedy, J. D.; Nestor, K.; Thornton-Pett, M.; Hermánek, S.; Jelinek, T.; Stibr, B. *J. Chem. Soc., Dalton Trans.* **1990**, 681.

(11) (a) Mashima, K.; Haraguchi, H.; Ohyoshi, A.; Sakai, N.; Takaya, H. *Organometallics* **1991**, *10*, 2731. (b) Cohen, S. A.; Bercaw, J. E. *Organometallics* **1985**, *4*, 1006.

resonance (δ 1.6, 1B) does not split in the ^1H -coupled ^{11}B NMR spectrum.¹² These data establish that **7** contains one type of chemically unique Cp*, BCHMeO-, and dicarbollide group and indicate that the sides of the dicarbollide ligands are inequivalent.

The 2D-NOESY spectrum of **7** (C_6D_6) provides important clues to the structure of this compound. Key NOESY correlations for **7** are indicated in Figure 2. A strong NOESY correlation between the -BCHMeO-hydrogen and one dicarbollide CH (Ha, δ 0.4) is observed, which establishes that the -CHMeO- bridge is attached to the dicarbollide cage through a lateral C_2B_3 boron (B4 or B7) and that the BCHMeO and Ha hydrogens are arranged in a syn fashion. Additionally, a NOESY correlation is observed between the -BCHMeO- and Cp* hydrogens. As a -BCHMeO-/Cp* NOESY correlation is *not* observed in monomeric **6**, the -BCHMeO-/Cp* correlation in **7** implies that the -BCHMeO- hydrogen on one metallocene unit must be close in space to the Cp* group of the other metallocene unit. These NOESY results are consistent with the structure shown in Figure 2. Additionally, NOESY correlations are observed between the Cp* hydrogens and *both* dicarbollide CH hydrogens. In the dimeric structure in Figure 2, Hb is close in space to the Cp* group on the same monomer unit (due to the restricted rotation of the dicarbollide cage) and Ha is close in space to the Cp* group on the other monomer unit.¹³ The configuration of each Cp*(η^5 : η^1 -4-CHMeO- $\text{C}_2\text{B}_9\text{H}_{10}$)Ti unit in **7** may be denoted by the descriptor "4,*S*" (enantiomer = *7,R*) where the first entry defines the site of attachment of the bridge to the cage and, hence, the configuration of the cage and the second entry defines the configuration of the bridge carbon. It is remarkable that only a single diastereomer of **7** is observed.

Reaction of 7 with Lewis Bases. Synthesis of Cp*(η^5 : η^1 -4-CHMeO- $\text{C}_2\text{B}_9\text{H}_{10}$)Ti(NCMe) (9**).** One interesting feature of the ^1H NMR spectrum of **7** is that the dicarbollide CH resonance (Ha) which exhibits a NOESY correlation with the Cp* resonance appears at high field in noncoordinating solvents (toluene- d_6 , δ 0.41). This effect is presumed to result from anisotropic shielding of Ha by the Cp* ring. The Ha resonance moves upfield to -0.12 at -80 °C, which is consistent with the increased extent of dimerization of **7** expected at the lower temperature. However, the Ha resonance moves downfield to the normal range (ca. δ 1.5–3.0) in the presence of Lewis bases or coordinating solvents (L), suggesting that monomeric Cp*(η^5 : η^1 -4-CHMeO- $\text{C}_2\text{B}_9\text{H}_{10}$)-TiL adducts are formed. For example, the Ha resonance of **7** appears at δ 1.6 in the presence of CO (ca. 1 atm, toluene- d_6) and at δ 2.2 ppm (-70 °C) in THF- d_6 .¹⁴ Treatment of a mixture of **6** and **7** with excess CH_3CN followed by crystallization of the crude product from CH_3CN yields the acetonitrile adduct Cp*(η^5 : η^1 -4-

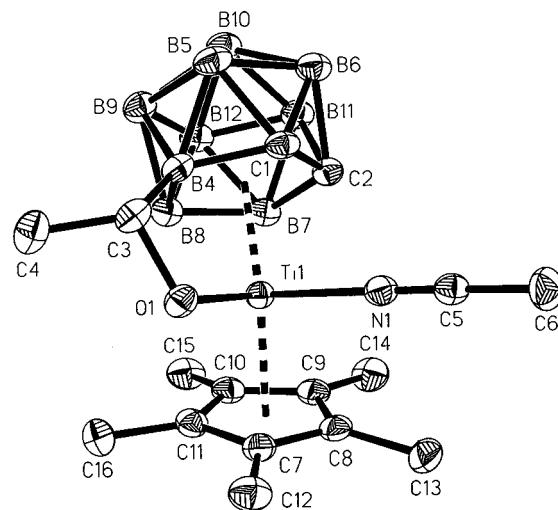


Figure 3. Molecular structure of Cp*(η^5 : η^1 -4-CHMeO- $\text{C}_2\text{B}_9\text{H}_{10}$)Ti(NCMe) (**9**).

Table 2. Selected Bond Lengths (Å) and Angles (deg) for Cp*(η^5 : η^1 -4-CHMeO- $\text{C}_2\text{B}_9\text{H}_{10}$)Ti(CH₃CN) (9**)^a**

Ti(1)-cnt(Dc)	1.961	Ti(1)-cnt(Cp*)	2.113
Ti(1)-O(1)	1.869(2)	Ti(1)-N(1)	2.174(2)
Ti(1)-C(11)	2.388(2)	Ti(1)-B(4)	2.397(2)
Ti(1)-C(7)	2.415(2)	Ti(1)-B(8)	2.417(2)
Ti(1)-C(10)	2.422(2)	Ti(1)-C(1)	2.422(2)
Ti(1)-C(8)	2.485(2)	Ti(1)-C(2)	2.462(2)
Ti(1)-C(9)	2.465(2)	Ti(1)-B(7)	2.454(2)
B(4)-C(3)	1.581(3)	C(5)-C(6)	1.460(3)
C(3)-O(1)	1.470(2)	N(1)-C(5)	1.141(3)
C(3)-C(4)	1.520(3)		
cnt(Cp*)-Ti-cnt(Dc)	140.4	cnt(Dc)-Ti-O(1)	102.6
cnt(Cp*)-Ti-O(1)	105.0	cnt(Dc)-Ti-N(1)	105.0
cnt(Cp*)-Ti-N(1)	100.4	C(4)-C(3)-B(4)	115.8(2)
O(1)-Ti(1)-N(1)	95.02(7)	C(3)-O(1)-Ti(1)	110.5(1)
O(1)-C(3)-B(4)	99.6(2)	O(1)-C(3)-C(4)	109.2(2)

^a The centroids of the Cp* and dicarbollide rings are denoted by cnt(Cp*) and cnt(Dc), respectively.

CHMeO- $\text{C}_2\text{B}_9\text{H}_{10}$)Ti(NCMe) (**9**) as a yellow crystalline solid, which contains 1 equiv of occluded acetonitrile (eq 1).

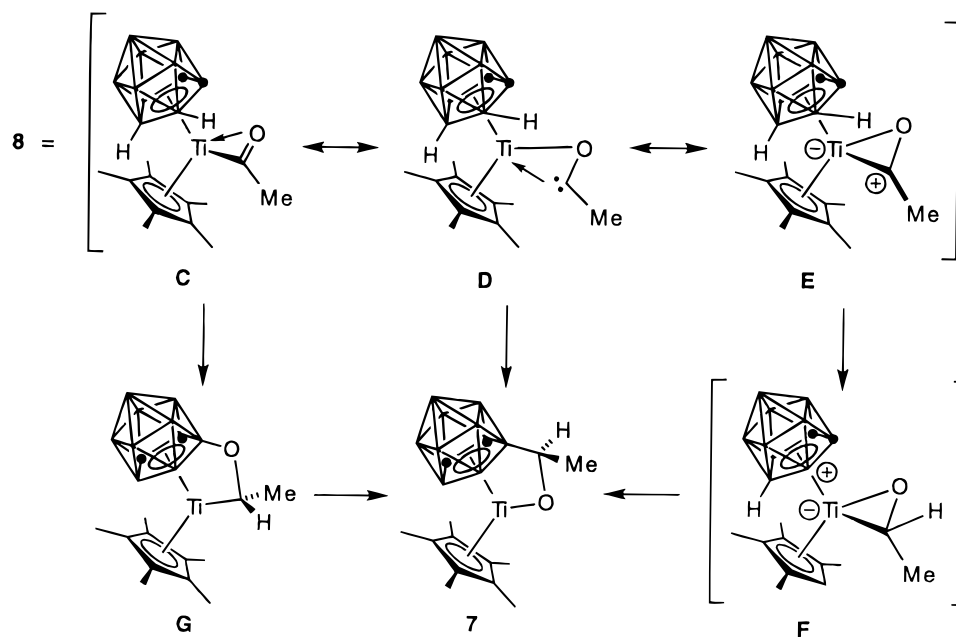
The molecular structure of **9** was determined by X-ray crystallography and is shown in Figure 3. Important bond distances and bond angles are given in Table 2. Compound **9** adopts a four-coordinate bent-metallocene structure in which the TiOCHMe- bridge is attached to a lateral boron (B4) of the C_2B_3 face. The centroid-Ti-centroid angle (140.4°) is smaller than that of **6**, and the Ti-(Cp* centroid) and Ti-(dicarbollide centroid) distances (2.11, 1.96 Å) are greater than those of **6**, as expected due to the higher coordination number of **9**. The bridge structure is similar to that of **6**; the B(4)-C(3) bond is directed 41.1° out of the C_2B_3 plane toward Ti, the O(1)-C(3)-B(4) angle (99.6(2)°) is reduced from the normal tetrahedral value, and the C(3)-O(1) distance is slightly longer than normal (1.470(2) Å). The acetonitrile and alkoxide ligands lie in the plane between the dicarbollide and Cp* ligands (angle between (Cp* centroid)-Ti-(dicarbollide centroid) and O(1)-Ti-N(1) planes = 92.5°), and the O(1)-Ti-N(1) angle in **9** (95.02(7)°) is normal for a d^0 metallocene. Overall, the structure of **9** is very similar to that of Cp*(η^5 : η^1 - $\text{C}_2\text{B}_9\text{H}_{11}$)Ti(NC=CMe₂)(CH₃CN) (**10**), the acetonitrile adduct of **4**.^{1a} The Ti-(dicarbollide centroid) distance

(12) The ^{11}B - ^{11}B COSY spectra (C_6D_6 , THF- d_6) of **7** were uninformative due to overlapping resonances. The B4 resonance of **7** is partially overlapped with another resonance in C_6D_6 .

(13) For comparison, dicarbollide CH/Cp* NOESY correlations are not observed for related compounds containing unlinked dicarbollide ligands, such as **5** and Cp*(η^5 :*R*-1,2- $\text{C}_2\text{B}_9\text{H}_{10}$)HfC≡CMe (R = CHMe-(3,5-Me₂-2-cyclopentadienyl)), see ref 1a, f.

(14) In THF- d_6 , the dicarbollide CH resonances are broadened into the base line at room temperature.

Scheme 3



of **9** (1.96 Å) is shorter than that of **10** (2.02 Å) as a result of a shortening of the Ti–B(4), Ti–B(8), and Ti–C(1) bonds due to the effect of the bridge. The relative stereochemistry of the carborane cage, the linker carbon, and the Ti center in **9** are consistent with the stereochemistry of **7** deduced by NMR.

The low-temperature (–90 °C) ¹H NMR spectrum of **9** contains one Cp* resonance, one set of –BCHMeO– resonances, two dicarbollide CH resonances, and a resonance for coordinated CH₃CN that is shifted from that of free CH₃CN. This spectrum establishes that **9** exists as a single diastereomer under these conditions; presumably, the metal configuration is the same as that observed in the solid state. Exchange of coordinated and free CH₃CN is slow at –90 °C but rapid on the NMR time scale at ambient temperature.

Discussion

The carbonylation of **1** most likely proceeds by initial formation of the acyl species **8** followed by net insertion of the acyl carbon into a B–H bond to produce **6** or **7**.¹⁵ Intermediate **8** was not observed but is expected to adopt an η²-acyl structure as do other electron-deficient early transition metal acyl species.¹⁶ The acyl bonding in **8** may be represented by the resonance forms C–E in Scheme 3, the latter two of which emphasize the electrophilic character of the acyl carbon center.¹⁷ The rearrangement to **6** or **7** involves nucleophilic attack of the central or a lateral B–H bond at the electrophilic acyl carbon. While the present results do not provide detailed mechanistic information, the geminal addition may result from stepwise H[–] transfer followed by B–C bond formation (i.e., E → F → 7) or from initial 1,2-

B–H addition to the C=O bond followed by rearrangement (i.e., C → G → 7). Alternatively, the rearrangement of **8** may be viewed as a carbene-like insertion of the acyl carbon into the B–H bond (i.e., D → 7). The formation of **6** and **7** is, thus, similar to the reactions of other early transition metal η²-acyl complexes with nucleophilic hydride species, which in many cases yield MOCHRM' products.¹⁸ For example, the reaction of Cp₂Zr(η²-COMe)Me with Cp₂ReH yields Cp₂Zr(Me)-OCHMeReCp₂.¹⁹ The conversion of putative intermediate **8** to **6** or **7** is also similar to the formal insertions of alkylidene ligands into dicarbollide B–H bonds observed for late transition metal dicarbollide complexes.²⁰ For example, protonation of the anionic alkylidyne complex (η⁵-1,2-Me₂-C₂B₉H₉)W(CO)₂(=CAr)[–] in the presence of CO yields (η⁵-1,2-Me₂-8-CH₂Ar-C₂B₉H₈)W(CO)₄ via insertion of the initially formed W=CHAr alkylidene group into the B8–H bond of the dicarbollide ligand. Finally, the chemistry observed here is related to the rearrangement of {H₂B(3,5-Me₂-pyrazoyl)₂}Mo(CO)₂(PMe₃){η²-C(=O)Me} to {HB(3,5-Me₂-pyrazoyl)₂(OCHMe)}Mo(CO)₂(PMe₃), which proceeds by 1,2-B–H addition to the acyl C=O bond.²¹

The current results show that B–H bond reactivity is an important feature of d⁰ metal dicarbollide com-

(15) The possibility that **1** reacts with CO at a B–H bond to yield a B–C(=O)H intermediate which rearranges to **6** or **7** by nucleophilic attack of the Ti–Me group at the acyl carbon is very unlikely because reactions of **1** with other unsaturated substrates occur at the Ti–Me bond, see ref 1a.

(16) Durfee, L. D.; Rothwell, I. P. *Chem. Rev.* **1988**, *88*, 1059.

(17) Tatsumi, K.; Nakamura, A.; Hofmann, P.; Stauffert, P.; Hoffmann, R. *J. Am. Chem. Soc.* **1985**, *107*, 4440.

(18) (a) Fachinetti, G.; Floriani, C.; Rosselli, A.; Pucci, S. *J. Chem. Soc., Chem. Commun.* **1978**, 269. (b) Gell, K. I.; Schwartz, J. *J. Organomet. Chem.* **1978**, *162*, C11. (c) Wolczanski, P. T.; Bercaw, J. E. *Acc. Chem. Res.* **1980**, *13*, 121. (d) Maatta, E. A.; Marks, T. J. *J. Am. Chem. Soc.* **1981**, *103*, 3576. (e) Erker, G. *Acc. Chem. Res.* **1984**, *17*, 103.

(19) Marsella, J. A.; Huffman, J. C.; Folting, K.; Caulton, K. G. *Inorg. Chim. Acta* **1985**, *96*, 161.

(20) (a) Jelliss, P. A.; Stone, F. G. A. *J. Organomet. Chem.* **1995**, *500*, 307. (b) Brew, S. A.; Stone, F. G. A. *Adv. Organomet. Chem.* **1993**, *35*, 135. (c) Brew, S. A.; Devore, D. D.; Jenkins, P. D.; Pilotti, M. U.; Stone, F. G. A. *J. Chem. Soc., Dalton Trans.* **1992**, 393. (d) Brew, S. A.; Carr, N.; Jeffery, J. C.; Pilotti, M. U.; Stone, F. G. A. *J. Am. Chem. Soc.* **1992**, *114*, 2203. (e) Brew, S. A.; Stone, F. G. A. *J. Chem. Soc., Dalton Trans.* **1992**, 867. (f) Dossett, S. J.; Li, S.; Mullica, D. F.; Sappenfield, E. L.; Stone, G. A. *J. Chem. Soc., Dalton Trans.* **1993**, 3551. (g) Anderson, S.; Jeffery, J. C.; Liao, Y.; Mullica, D. F.; Sappenfield, E. L.; Stone, F. G. A. *Organometallics* **1997**, *16*, 958.

(21) Pizzano, A.; Sánchez, L.; Gutiérrez, E.; Monge, A.; Carmona, E. *Organometallics* **1995**, *14*, 14.

plexes. This observation and earlier observations of B–H···M agostic interactions and dicarbollide C–H activation reactions show that group 4 metal (C₅R₅)-(C₂B₉H₁₁)MR complexes are multifunctional systems which contain electrophilic metal centers (M), nucleophilic hydrocarbyl groups (R), and potentially reactive dicarbollide B–H and C–H bonds.¹ The B–H activation reaction leading to **6** and **7** complicates the possibility of using **1** to mediate alternating alkyne/CO insertion reactions. However, as reported elsewhere, the B–H reactivity of (C₅R₅)(C₂B₉H₁₁)HfR species gives rise to unique properties in the catalytic dimerization of terminal alkynes.^{1f}

Experimental Section

General Procedures. All manipulations were performed using vacuum-line or Schlenk techniques or in a glovebox under a purified N₂ atmosphere. Solvents were distilled from the appropriate drying/deoxygenating agents and stored under vacuum or N₂ prior to use. Toluene, benzene, hexanes, pentane, and THF were distilled from Na/benzophenone. Acetonitrile was distilled from P₂O₅ and then from activated molecular sieves. C₂B₉H₁₃, Cp*TiMe₃, and Cp*(C₂B₉H₁₁)TiMe were synthesized by literature procedures.^{1,22} NMR spectra were recorded on a Bruker AMX-360 instrument at 25 °C in sealed or Teflon-valved tubes, unless indicated otherwise. ¹H and ¹³C NMR chemical shifts are reported versus Me₄Si and were determined by reference to the residual solvent peaks. Coupling constants are reported in hertz. The ¹H NMR spectra contain broad B–H resonances in the range δ 0–4, which are not reported. ¹¹B NMR spectra were referenced to an external BF₃·Et₂O standard in C₆D₆. Elemental analyses were performed by E&R Microanalytical Laboratory, Inc.

Synthesis of **6 and **7**.** A toluene solution (1 mL) of C₂B₉H₁₃ (127 mg, 0.947 mmol) was added to a pentane solution (3 mL) of Cp*TiMe₃ (229 mg, 1.00 mmol) dropwise at 23 °C. The reaction mixture was stirred for 10 min, and the volatiles were removed under vacuum. The residue was washed with pentane (4 × 0.3 mL), yielding a deep red solid. Toluene (15 mL) was added, and the deep red solution was degassed and exposed to CO (1 atm) for 20 min at 23 °C. The solution was filtered, and the volatiles were removed from the filtrate under vacuum, yielding a deep brown sticky residue. The residue was triturated with pentane (2 × 5 mL) and dried under vacuum, affording a deep brown powder (292 mg, 93.3%). The ¹H NMR spectrum indicated that the **6**:**7** ratio was ca. 1:4. This product was washed with hexanes, yielding an analytically pure sample of a 1:4 **6**:**7** mixture (241 mg, 77.0%). The use of ¹³CO in this reaction yields a mixture of **6**-¹³C₁ and **7**-¹³C₁, each labeled in the alkoxide carbon position.²³ Anal. Calcd for C₁₄H₂₉B₉O₁Ti: C, 46.90; H, 8.15. Found: C, 46.84; H, 8.25.

Isolation of **6.** Benzene (50 mL) was added to a 1:1 mixture of **6** and **7** (495 mg, 1.38 mmol). Acetonitrile (0.7 mmol) was added to the benzene solution by vacuum transfer

at –196 °C. The mixture was stirred for 2 days at 23 °C and filtered through Celite. The volatiles were removed from the filtrate under vacuum, and the residue was triturated with hexanes, yielding a brown solid (310 mg). Toluene (10 mL) was added to the solid, and the solution was kept in a –40 °C freezer overnight, yielding a deep brown solution and a precipitate. The mixture was filtered. The filtrate was taken to dryness under vacuum, yielding a sticky solid, which was extracted with benzene/hexanes (1:4, 5 mL). The extract was concentrated to ca. 1 mL and maintained at 23 °C for 4 days, yielding deep red/black crystals of **6**, which were used for the X-ray analysis.

NMR Data for **6.** ¹H NMR (C₆D₆): δ 6.33 (br q, *J* = 6.7, 1H, CHMe), 3.34 (br s, 1H, dicarbollide CH), 3.26 (br s, 1H, dicarbollide CH), 1.81 (d, *J* = 6.7, 3H, CHMe), 1.57 (s, 15H, C₅Me₅). {¹H}–¹¹B NMR (C₆D₆): see Figure 1 for numbering system: δ 11.9 (1B, B8), 4.8 (1B, B4 or B4'), 2.6 (1B, B4' or B4), –2.7 (2B, B9 and B9'), –10.8 (1B, B6), –12.3 (2B, B5 and B5'), –20.1 (1B, B10). ¹¹B NMR (C₆D₆): δ 11.9 (s, 1B), 4.8 (d, *J*_{BH} = 136, 1B), 2.6 (d, *J*_{BH} = 136, 1B), –2.7 (d, *J*_{BH} = 136, 2B), –10.8 (d, partially obscured, *J*_{BH} ≈ 160, 1B), –12.3 (d, partially obscured, *J*_{BH} ≈ 149, 2B), –20.1 (d, *J*_{BH} = 136, 1B). ¹¹B–¹¹B COSY (correlations and relative intensities): B8–(B4 (s), B4' (s)), B8–(B9, B9' (m)), (B4, B4')–(B9, B9' (m)), (B9, B9')–B10 (w), (B5, B5')–B10 (vw). The expected B6–(B5, B5') correlation was not observed, clearly due to partial overlap of these resonances. {¹H}–¹³C NMR (CD₂Cl₂): δ 131.2 (C₅Me₅), 86 (br, B–CHMe), 59.2 (br, dicarbollide CH, 2C), 21.3 (CHMe), 11.5 (C₅Me₅).

NMR Data for **7.** ¹H NMR (toluene-*d*₆): 5.61 (q, *J* = 7.2, 1H, CHMe), 2.68 (br, 1H, dicarbollide CH), 1.75 (d, *J* = 7.2, 3H, CHMe), 1.70 (s, 15H, C₅Me₅), 0.41 (br s, 1H, dicarbollide CH). ¹H NMR (toluene-*d*₈, –80 °C): δ 5.77 (br s, 1H, CHMe), 2.64 (br s, 1H, dicarbollide CH), 2.0 (br s, 3H, CHMe), 1.62 (s, 15H, C₅Me₅), –0.12 (br s, 1H, dicarbollide CH). ¹H NMR (THF-*d*₆, –70 °C): δ 5.19 (br q, *J* = 6.1, 1H, CHMe), 2.52 (br s, 1H, dicarbollide CH), 2.19 (br s, 1H, dicarbollide CH), 2.10 (s, 15H, C₅Me₅), 1.04 (d, *J* = 6.5, 3H, CHMe). The assignments of the dicarbollide CH resonances were confirmed by a ¹H–¹H COSY experiment. {¹H}–¹¹B NMR (C₆D₆): δ 20.7 (1B), 0.2 (2B), –1.3 (1B), –2.8 (1B), –9.0 (2B), –13.3 (1B), –19.7 (1B). ¹¹B NMR (C₆D₆): δ 20.7 (d, *J*_{BH} = 120, 1B), 0.2 (s and d, 2B, partially obscured), –1.3 (d, 1B, partially obscured), –2.8 (d, *J*_{BH} ≈ 141, 1B), –9.0 (d, *J*_{BH} ≈ 129, 2B), –13.3 (d, obscured, 1B), –19.7 (d, *J*_{BH} ≈ 136, 1B). {¹H}–¹³C NMR (CD₂Cl₂): δ 133.1 (C₅Me₅), 83 (br, CHMe), 62 (CH, dicarbollide), 60 (CH, dicarbollide), 19.6 (CHMe), 12.0 (C₅Me₅).

Cp*(η^5 : η^1 -4-C₂B₉H₁₀-CHMeO)Ti(NCMe) (9**).** Acetonitrile (1 mL) was added by vacuum transfer to a 1:5 mixture of **6** and **7** (140 mg). The mixture was stirred for 3.5 h at 23 °C, and the volatiles were removed under vacuum. The residue was washed with pentane (3 × 5 mL), yielding a yellow solid (126 mg). The ¹H NMR spectrum of the yellow solid indicated that it contained **9** and a minor species, which is presumed to be the acetonitrile adduct of **6** (**6**·NCMe), in a 5:1 ratio, and free MeCN (ca. 1 equiv vs **9**).²⁴ Yellow crystals of **9**·MeCN suitable for X-ray crystallography were grown by cooling a solution of **6** and **7** (1:5 ratio, 44 mg) in acetonitrile (0.4 mL) to –35 °C overnight without agitation.

NMR Data for **9.** ¹H NMR (CD₂Cl₂, –90 °C): δ 4.91 (br q, *J* = 7.2, 1H, CHMe), 2.92 (br s, 1H, dicarbollide CH), 2.46 (s, 3H, Ti–NCMe), 1.98 (s, 15H, C₅Me₅), 1.73 (br s, 1H, dicarbollide CH), 0.90 (d, *J* = 7.2 Hz, 3H, CHMe); the resonance for free NCMe is observed at δ 1.86 at this temperature. The assignments of the dicarbollide CH resonances were confirmed by ¹H–¹H COSY experiment. ¹³C NMR (CD₂Cl₂, –60 °C): δ

(24) ¹H NMR of **6** (CD₂Cl₂): δ 5.88 (br q, *J* = 6, 1H, CHMe), 3.72 (br s, 1H, dicarbollide CH), 3.63 (br s, 1H, dicarbollide CH), 2.17 (s, 15H, C₅Me₅), 1.47 (d, *J* = 7, 3H, CHMe). ¹H NMR of **6**·NCMe (CD₂Cl₂) in the presence of excess MeCN: δ 5.6 (br, 1H, CHMe), 1.2 (br, 3H, CHMe).

(22) (a) Uhrhammer, R.; Crowther, D. J.; Olson, J. D.; Swenson, D. C.; Jordan, R. F. *Organometallics* **1992**, *11*, 3098 and references therein. (b) Mena, M.; Royo, P.; Serrano, R.; Pellinghelli, M. A.; Tiripicchio, A. *Organometallics* **1989**, *8*, 476.

(23) Data for **6**-¹³C₁: ¹H NMR (C₆D₆) δ 6.3 (dq, *J*_{CH} = 139, *J*_{HH} = 7, 1H, CHMe), 3.44 (br s, 1H, dicarbollide CH), 3.37 (br s, 1H, dicarbollide CH), 1.8 (br, overlapped with resonance of **7**-¹³C₁, 3H, CHMe), 1.6 (s, 15H, C₅Me₅); Gated {¹H}–¹³C NMR (C₆D₆) δ 130.8 (C₅Me₅), 86.5 (br, CHMe), 62.8 (d, *J*_{CH} = 172, two dicarbollide C overlapped), 22.3 (qd, *J*_{CH} = 127, *J*_{CC} = 35, CHMe), 11.6 (q, *J*_{CH} = 128, C₅Me₅). Data for **7**-¹³C₁: ¹H NMR (C₆D₆) δ 5.6 (dq, *J*_{CH} = 139, *J*_{HH} = 7, 1H, CHMe), 2.7 (s, dicarbollide CH, 1H), 1.8 (br, overlapped, 3H, CHMe), 1.7 (s, 15H, C₅Me₅), 0.5 (br, 1H, dicarbollide CH); Gated {¹H}–¹³C NMR (C₆D₆) δ 132.2 (C₅Me₅), 83.9 (br, CHMe), 60.9 (d, *J*_{CH} = 178, dicarbollide C), 59.3 (d, *J*_{CH} = 175, dicarbollide C), 20.7 (qd, *J*_{CH} = 126, *J*_{CC} = 35, CHMe), 12.0 (q, *J*_{CH} = 128, C₅Me₅).

Table 3. Crystal Data and Structure Refinement for **6**·C₆H₆ and **9**·CH₃CN

compd	6 ·C ₆ H ₆	9 ·CH ₃ CN
empirical formula	C ₂₀ H ₃₅ B ₉ OTi	C ₁₈ H ₃₅ B ₉ N ₂ OTi
fw	436.67	440.67
crystal size (mm)	0.40 × 0.33 × 0.24	0.40 × 0.35 × 0.35 mm
color/shape	red prism	yellow block
space group	<i>Cmca</i>	<i>P</i> $\bar{1}$
<i>a</i> (Å)	13.950(5)	8.7624(2)
<i>b</i> (Å)	18.104(3)	10.1559(2)
<i>c</i> (Å)	19.466(8)	15.4810(1)
α (deg)		101.601(1)
β (deg)		92.986(1)
γ (deg)		114.385(1)
<i>V</i> (Å ³)	4916(3)	1214.95(4)
<i>Z</i>	8	2
density (calcd, Mg/m ³)	1.180	1.205
abs coeff (mm ⁻¹)	0.359	0.365
<i>F</i> (000)	1840	464
diffractometer	Enraf-Nonius CAD4	Siemens SMART Platform CCD
radiation, λ (Å)	0.710 73	0.710 73
<i>T</i> (K)	210(2)	173(2)
θ range (deg)	2.0–25.0	1.36–25.03
data collected	–13 ≤ <i>h</i> ≤ 13, –17 ≤ <i>k</i> ≤ 17, –18 ≤ <i>l</i> ≤ 18	–10 ≤ <i>h</i> ≤ 10, –12 ≤ <i>k</i> ≤ 11, 0 ≤ <i>l</i> ≤ 18
no. of reflns	12 210	6156
no. of unique reflns	1796 (<i>R</i> _{int} = 0.0739)	4163 (<i>R</i> _{int} = 0.0182)
structure solution	direct methods	direct methods
refinement	full-matrix least-squares on <i>F</i> ²	full-matrix least squares on <i>F</i> ²
abs corr	ψ scans	SADABS
max and min transmission	0.999 and 0.688	1.000 and 0.756
data/restraints/params	1796/43/190	4163/0/332
goodness-of-fit on <i>F</i> ²	0.897	1.044
<i>R</i> indices (<i>I</i> ≥ 2 σ (<i>I</i>)) ^a	<i>R</i> 1 = 0.0664, <i>wR</i> 2 = 0.1432	<i>R</i> 1 = 0.0406, <i>wR</i> 2 = 0.1056
<i>R</i> indices (all data)	<i>R</i> 1 = 0.1966, <i>wR</i> 2 = 0.2017	<i>R</i> 1 = 0.0499, <i>wR</i> 2 = 0.1117
largest diff peak and hole (e/Å ³)	0.253 and –0.301	0.272 and –0.367

^a *R*1 = $\sum |F_o| - |F_c| / \sum |F_o|$; *wR*2 = $[\sum (w_i(F_o^2 - F_c^2)^2) / \sum (w_i(F_o^2)^2)]^{1/2}$.

131.3 (NCMe), 127.6 (C₅Me₅), 80.8 (br, *J*_{CH} = 136, CHMe), 55.0 (br, 2 CH, dicarbollide), 19.2 (*J*_{CH} = 126, CHMe), 12.8 (*J*_{CH} = 126, C₅Me₅), 4.9 (*J*_{CH} = 138, NCMe). {¹H}–¹¹B NMR of **9**·(MeCN) (CD₂Cl₂): δ 10.1 (1B), –0.1 (1B), –3.04 (2B), –5.0 (1B), –10.9 (1B), –14.7, –15.7 (3B, partially overlapped).

Molecular Weight Measurement of 7. The molecular weight of **7** was determined by cryoscopy in benzene.²⁵ A mixture of **6** and **7** (1:4 ratio, 17.9 mg) was dissolved in benzene (1.7769 g). Since **6** and **7** have the same empirical formula, the weight of **6** is $17.9 \times 1/5 = 3.6$ mg, and the weight of **7** is $17.9 - 3.6 = 14.3$ mg. The calculated molality for **6** (*m*₆) is 0.0056, assuming **6** is a monomer in benzene solution as it is in the solid state. The total molality for **6** and **7** (*m* = *m*₆ + *m*₇) was determined to be 0.0194 by cryoscopy. The molality of **7** is given by *m*₇ = 0.0194 – *m*₆ = 0.0138. The calculated molecular weight for **7** is, therefore, 584(30), which is intermediate between values expected for monomeric (358.5) and dimeric (717.0) structures.

X-ray Crystallographic Analysis of 6·C₆H₆. Crystallographic details are summarized in Table 3. The subject molecule is situated on a crystallographic mirror plane that passes through C(11), C(16), B(6), B(10), and Ti(1). Crystallographic symmetry requires that the O(1), C(6), (C7), and B(8) atoms to be disordered (50%), i.e., both enantiomers of the racemate alternately occupy the same crystallographic site. The dicarbollide hydrogen atom coordinates were refined with restraints. The B–H and C–H distances were restrained to be the same, the B–B–H angles were restrained to be the same for a given B–H group, and the same isotropic thermal parameter was used (and refined) for all C₂B₉ hydrogen atoms. All other hydrogen atoms were included with the riding model. The methyl hydrogen atoms were allowed to rotate about the C–H bond, and a refined isotropic thermal parameter was given to each set of methyl H atoms. The C(16) hydrogen

atoms are disordered (50%). A molecule of benzene (solvent) is situated near a crystallographic 2-fold axis and is necessarily disordered. High thermal motion was apparent for the benzene. The benzene was modeled with two rigid groups (C–C = 1.39 Å, C–C–C = 120°, riding H atoms) represented by atoms C51–C56 (occupancy = 0.44(4)) and C61–C66 (occupancy = 0.56(4)). Individual isotropic thermal parameters were assigned to all partial C atoms, and those for C atoms within 0.5 Å of another were restrained to be similar in magnitude. Riding model parameters are as follows: C–H = 0.93 Å for sp² C atoms; C–H = 0.96–0.98 Å for sp³ C atoms; *U*_{iso} (H) = 1.2*U*_{iso}(C).

X-ray Crystallographic Analysis of 9·CH₃CN. A successful direct-methods solution was calculated which provided most of the non-hydrogen atoms from the *E*-map. Several full-matrix least-squares/difference Fourier cycles were performed, which located the remainder of the non-hydrogen atoms. All non-hydrogen atoms were refined with anisotropic displacement parameters. All hydrogen atoms were placed in ideal positions and refined as riding atoms with individual isotropic displacement parameters. A molecule of CH₃CN of crystallization is present.

Acknowledgment. This work was supported by the National Science Foundation (Grant No. CHE-9413022).

Supporting Information Available: Tables of atomic coordinates and equivalent isotropic displacement parameters, anisotropic displacement parameters, bond lengths and bond angles, and hydrogen atom coordinates and isotropic displacement factors for **6**·C₆H₆ and **9**·CH₃CN (16 pages). Ordering information is given on any current masthead page.

(25) Shriver, D. F.; Drezdson, M. A. *The Manipulation of Air-Sensitive Compounds*, 2nd ed.; John Wiley & Sons: New York, 1986; p 38 and references therein.